Contents lists available at ScienceDirect

Materials Science & Engineering C

journal homepage: www.elsevier.com

Investigation of cell adhesion in chitosan membranes for peripheral nerve regeneration

Cristiana R. Carvalho [a, b], Rita López-Cebral [a, b], Joana Silva-Correia [a, b], Joana M. Silva [a, b], João F. Mano [a, b], Tiago H. Silva [a, b], Thomas Freier [c], Rui L. Reis [a, b], Joaquim M. Oliveira [a, b, *, 1]

[a] *3B's Research Group - Biomaterials, Biodegradables and Biomimetics, University of Minho, Headquarters of the European Institute of Excellence on Tissue Engineering and Regenerative Medicine, AvePark – Parque de Ciência e Tecnologia, 4805-017, Barco, Guimarães, Portugal*
[b] *ICVS/3B's - PT Government Associate Laboratory, Braga, Guimarães, Portugal*
[c] *MEDOVENT GmbH, Friedrich-Koenig-Str. 3, D-55129 Mainz, Germany.*

ARTICLE INFO

Article history:
Received 4 July 2016
Received in revised form 13 October 2016
Accepted 24 November 2016
Available online xxx

Keywords:
Peripheral nerve injuries
Biomaterials
Chitosan
Degree of acetylation
Schwann cells
L929 mouse fibroblast cells

ABSTRACT

Peripheral nerve injuries have produced major concerns in regenerative medicine for several years, as the recovery of normal nerve function continues to be a significant clinical challenge. Chitosan (CHT), because of its good biocompatibility, biodegradability and physicochemical properties, has been widely used as a biomaterial in tissue engineering scaffolding. In this study, CHT membranes were produced with three different Degrees of Acetylation (DA), envisioning its application in peripheral nerve regeneration. The three CHT membranes (DA I: 1%, DA II: 2%, DA III: 5%) were extensively characterized and were found to have a smooth and flat surface, with DA III membrane having slightly higher roughness and surface energy. All the membranes presented suitable mechanical properties and did not show any signs of calcification after SBF test. Biodegradability was similar for all samples, and adequate to physically support neurite outgrowth. The *in vitro* cell culture results indicate selective cell adhesion. The CHT membranes favoured Schwann cells invasion and proliferation, with a display of appropriate cytoskeletal morphology. At the same time they presented low fibroblast infiltration. This fact may be greatly beneficial for the prevention of fibrotic tissue formation, a common phenomenon impairing peripheral nerve regeneration. The great deal of results obtained during this work permitted to select the formulation with the greatest potential for further biological tests.

© 2016 Published by Elsevier Ltd.

1. Introduction

Peripheral nerves transmit information from the central nervous system to the remaining body parts, also transferring sensory information the other way around. Accordingly, lesions at this level can be highly harmful, causing life-long disabilities, commonly accompanied by pain. Peripheral nerve injuries (PNI) arise from different situations and pathologies, such as trauma, congenital birth defects or surgical complications [1]. Indeed, it has been reported that about 3% of trauma patients are affected by PNI [2] and these statistics are underestimated, as only traumatic injuries that reach the health care system are included [3]. Overall, more than half a million peripheral nerve injury cases are annually reported worldwide [4].

At present, nerve autografting is the most effective technique for nerve repair. Still, the outcomes are not satisfactory, often leading to incomplete functional recovery accompanied by tissue fibrosis formation and painful conditions. In addition, autografts have many drawbacks such as donor site morbidity and limited availability [5].

To improve PNI therapeutics, the production of bio-engineered scaffolds combining the knowledge about regeneration mechanisms, biomaterials and the novel biotechnological approximations, seem the only possible option leading to a successful outcome [6]. In previous works [7], it was asserted that the pathway leading to the development of successful neuronal scaffolds should start by the selection of the appropriate material, followed by its synthesis and characterization, and continued by *in vitro* testing. These analyses will reveal whether the material has the appropriate characteristics to be further studied.

It is also desired for the implantable scaffolds not only to hinder a fibrotic response, but to stop the formation of scar tissue. This will be mainly achieved by avoiding fibroblast adhesion [8]. Scar formation is important for avoiding wound extension, but excessive proliferation of this tissue as a response to nerve injury will result in inhibition of axon elongation [9]. On the other hand, it is essential for a peripheral nervous repair material to present good Schwann cell adhesion, as these cells are of fundamental importance for the nerve regeneration process to take place [10–12].

During the last decade scientists have been looking for the production of effective biodegradable artificial nerve guidance conduits (NGCs), without any significant success [13]. In this regard, increasing attention has been payed to chitosan (CHT) [14–17], due to the undisputable biomedical potential of this material, namely its polyelectrolyte properties [18], the presence of reactive functional groups, gel-forming ability [19], high adsorption capacity, complete

* Corresponding author at: ICVS/3B's - PT Government Associate Laboratory, Braga, Guimarães, Portugal.
Email address: miguel.oliveira@dep.uminho.pt (J.M. Oliveira)
[1] Postal address: 3B's Research Group - Biomaterials, Biodegradables and Biomimetics. AvePark, Zona Industrial de Gandra, AvePark – Parque de Ciência e Tecnologia, 4805-017 Barco – Guimarães.

http://dx.doi.org/10.1016/j.msec.2016.11.100
0928-4931/© 2016 Published by Elsevier Ltd.

UNCORRECTED PROOF

biodegradability [20], bacteriostatic [21] and fungistatic properties [22] or anti-tumour influence [23,24].

The degree of acetylation (DA) represents the proportion of *N*-acetyl-D-glucosamine units in the chitosan chain [25,26] and has an important impact on several physicochemical properties (*i.e.* viscosity, hydrophilicity, crystallinity, tensile strength, brittleness and degradation), as well as other important characteristics such as biocompatibility, biodegradation and cell interaction properties [25,27–29]. According to the literature, there are a few studies proving that, considering a wide range of DAs, lower acetylated materials lead to better results in terms of increased cell adhesion for PNR [26,30]. This statement has also been proved true in other regenerative medicine fields [20,25,29,31–33]. However, it has never been reported before how minor changes in the DAs would have a visible effect in cell adhesion, since a wider range and greater differences in the DAs are commonly studied. Also, it was verified that in the above mentioned previous studies, the lowest DA analyzed varied greatly, from 0.5% to 10%. Therefore, the statement found in the literature "DA close to zero leads to better results" is imprecise. Taking the previous information into account, the niche of DAs close to zero should be further investigated in order to shed light on their real suitability for peripheral nerve regeneration purposes.

In this work we hypothesize that even very small differences in low DAs might affect cellular behaviour and their regenerative potential. Therefore, we produced three different membranes using very low and similar DA CHTs as raw materials, DA I: 1% DA; DA II: 2% DA and DA III: 5% DA, and thoroughly investigated their surface and physicochemical properties. The biological performance of the developed CHT membranes was investigated using mouse lung L929 fibroblasts and human immortalized Schwann cells. This extensive characterization proved the potential of the membranes for PNR applications, leading to the revelation of the DA III membrane as the formulation with the highest PNR potential, consequently being this system the one selected for the future continuation of the present experimental work.

2. Experimental section

2.1. Materials

Highly purified chitosan powder (*Ki2*Med® LO_{80+}) with 5% DA was provided by Altakitin S.A. (Lisboa, Portugal). Chitosan powder with 2% and 1% DA, respectively, was produced from 5% DA chitosan by one or two hydrolysis steps in 40% sodium hydroxide for 2 h at 80 °C. Chitosan membranes with different degrees of acetylation (DA I: 1%, DA II: 2%, DA III: 5%) were produced and supplied by Medovent GmbH (Mainz, Germany) (Table 1). All chemicals for SBF preparation were obtained from Sigma-Aldrich, (Germany); Alamar Blue (AB) was purchased to Invitrogen™; CyQUANT® Cell Proliferation Assay Kit and Sodium Pyruvate 100 mM were obtained from Alfagene; Calcein AM and propidium iodide were obtained from Life Technologies, (CA, USA).

2.2. Methods

2.2.1. Membranes production

Briefly, highly purified chitosan powder with 1%, 2%, or 5% DA, respectively, was dissolved in 0.75% acetic acid to obtain a 1.5% solution, which was filtered and poured into Petri dishes, followed by drying at room temperature (RT) for 72 h. The resulting membranes were treated with a solution of ammonia in methanol/water [25], washed once with distilled water and dried for another 24 h. The membranes were cut into the required size and sterilized by electron beam.

The DA of the chitosan samples was determined using ^{1}HNMR spectroscopy, as previously described [26]. Briefly, samples were dissolved in a mixture of 0.25% DCl in D2O. The ^{1}HNMR spectra were recorded on Avance III HD 300 NMR-spectrometer (Bruker). The DA was calculated by comparing the integrated area of the H2-H6 group signal with that corresponding to the signal of the methyl group [26].

2.2.2. Physicochemical and surface characterization of membranes

2.2.2.1. Scanning Electron Microscopy (SEM)

The studied membranes were sputter coated with gold for the analyses of their surface morphology by means of SEM (model S360, Leica, Cambridge, England).

2.2.2.2. Atomic Force Microscopy (AFM)

The membranes surface roughness was analyzed using a Dimension 3000 Atomic Force Microscope (Digital Instruments, Santa Barbara, CA), on a 5 μm × 5 μm scan area. Contact mode was used with a Multimode (Veeco, USA) connected to a NanoScope III (Veeco, USA) having a contacting silicon nitride nanoprobe (model DNP, Bruker).

For this analysis, the membranes were tested under ambient conditions (dry) and after being immersed in Phosphate Buffer Saline (PBS) during 2 h to mimic physiological conditions (wet). The average surface roughness (Ra, nm) corresponding to the membranes in both dry and wet state was measured.

2.2.2.3. Contact angle measurements: wettability and surface energy determination

Differences in the wettability and surface free energy of the membranes were evaluated by means of contact angle measurements. Static contact angle measurements were carried out by the sessile drop method, using a contact angle meter (Goniometer OCA 15 +, Germany) in association with a high-performance image processing system (DataPhysics Instruments, Filderstadt, Germany).

During every determination, a motor driven syringe was used to deposit a drop of liquid over the membrane surface. The images corresponding to these drops were properly recorded and analyzed. The different determinations were performed at RT and in triplicate.

For the wettability determination, water was used. For the surface energy quantification, two different test liquids were required, one

Table 1
General characteristics of the chitosan used on the preparation of each one of the studied membranes. Surface characterization of the chitosan membranes: Mean Roughness (± standard deviation) in dry and wet state measured by Atomic Force Microscope analysis and water contact angle, surface energy and its components calculated by the WORK method.

Sample	Concentration of chitosan	DA	Average molecular weight	Mean roughness in dry state (Ra, nm)	Mean roughness in wet state (Ra, nm)	θ water (°)	SE (γ) mN m^{-1}	Disp (γ*d*) mN m^{-1}	Polar (γ*p*) mN m^{-1}
DA I	1.5%	1%	260 kDa	6.3 ± 0.48	7.3 ± 0.043	107.1 ± 0.33	32.07 ± 0.00	32.07 ± 0.01	0 ± 0.00
DA II	1.5%	2%	300 kDa	3.7 ± 0.82	5.1 ± 0.64	95.6 ± 4.49	31.53 ± 0.01	30.27 ± 0.00	1.26 ± 0.00
DA III	1.5%	5%	312 kDa	7.2 ± 0.24	7.5 ± 0.35	115.2 ± 1.96	35.22 ± 0.01	34.61 ± 0.01	0.61 ± 0.00

UNCORRECTED PROOF

apolar (diiodomethane) and one polar (water). The surface energy and its polar and dispersive components were calculated by means of the Owens, Wendt, Rabel and Kaeble (OWRK) method [34].

2.2.2.4. Fourier Transform Infrared Spectroscopy (FTIR)

The FTIR spectrum was obtained using Shimadzu IRPrestige 21 spectromer (Shimadzu, Europe). Samples were prepared as potassium bromide pellets at room temperature. The spectrum was collected by averaging 32 scans with a resolution of 4 cm^{-1}, corresponding to the 4000–400 cm^{-1} spectra region.

2.2.2.5. X-ray diffraction (XRD)

X-ray diffraction was used to determine the crystal structure of chitosan membranes. The diffraction pattern was measured using grazing incidence X-ray diffraction (GIXRD) with a diffractometer (Bruker D8 Discover) operated with accelerating voltage of 40 kV and a current of 40 mA.

The GIXRD scans were performed using Cu Kα radiation (wavelength = 0.154 nm), keeping a fixed incidence angle of 1° between the incident X-rays and specimen plane, while the detector was revolved between 5° and 40° with respect to the specimen, at a speed of 0.04°/1 s. The analyses were performed at room temperature.

2.2.2.6. Differential Scanning Calorimetry (DSC)

DSC analysis was performed on a DSC Q100 apparatus (TA Instruments Inc., USA). Samples were packed in a TA aluminum pan (3.5–4 mg sample weight), which was covered with a suitable aluminum cover. Both temperature and heat flux were previously calibrated with Indium. All samples were subjected to a first heating cycle, ranging from 0 °C to 200 °C at a rate of 10 °C/min, an isothermal step of 2 min followed by cooling to 0 °C and a second heating cycle, ranging from 0 °C to 350 °C at a rate of 1 °C/min. The measurements were performed under dry nitrogen atmosphere, at a flow rate of 50 mL/min. Only the behaviour showed by the membranes during the second heating cycle is presented.

2.2.2.7. Weight loss and water uptake

Weight loss and water uptake studies were performed by means of soaking 1 cm^2 chitosan membranes in PBS (pH 7.4) or PBS enriched with 13 mg/L of lysozyme for 30 days, at 37 °C. In the weight loss assay, to distinguish weight loss related to enzymatic degradation or simple hydrolysis, samples were also put in PBS without lysozyme for degradation assessment. At predefined time points (1 day, 15 days, 30 days) the swollen or degraded samples were extracted and the excess of water removed with filter paper. To minimize both enzyme loss of activity and possible changes in the pH, enzyme solution was changed every 3 days. To determine the degradation behaviour over time the samples were dried at RT and Eq. (1) was applied. The water uptake ability of the formulations was calculated according to Eq. (2).

$$\text{Weight loss } (\%) = (\text{MI} - \text{MF})/\text{MI} \times 100, \quad (1)$$

where MI is initial mass (before immersion in solution) and MF is final mass (after drying).

$$\text{Water uptake } (\%) = (\text{MW} - \text{MI})/\text{MI} \times 100 \quad (2)$$

where MW is the wet mass (wet, but after excessive water removal) and MI is initial mass.

Three replicates of each sample were studied and the average values considered.

2.2.2.8. Bioactivity

The aim of this assay was to discard the possibility of bioactivity occurring in the developed membranes, as this is a completely undesirable phenomenon in the context of PNR. For the *in vitro* bioactivity tests an acellular Simulated Body Fluid (SBF) (1.0 ×) was prepared as described elsewhere [35], containing the same ions as human blood plasma, at a nearly equal concentration. Sample membranes of 1 cm^2 were cut from the original processed membranes and immersed in freshly prepared SBF for 1, 15 and 30 days at 37 °C. Upon removal from SBF the samples were rinsed with distilled water and left to dry at RT. Finally, the presence/absence of a calcium-phosphate layer on their surface was determined using Scanning Electron Microscopy and Energy-Dispersive Spectroscopy (SEM/EDS) (Leica Cambridge S 360) at an accelerated voltage of 15 kV. Before SEM analyses, the membranes were gold coated at 6 mA, by using a Hitachi coater, in contraposition to dry membranes, that did not undergo this assay (controls).

2.2.2.9. Mechanical properties

The viscoelastic measurements were performed using a Tritec 2000B DMA (Triton Technology, UK). For this purpose, 5 mm width membrane samples were cut out and immersed in PBS overnight, at 37 °C. During the DMA analysis the samples were also immersed in PBS, in order to keep the physiological-like-state. Experiments were carried out under the tensile mode, following cycles of increasing frequency, from 0.1 to 20 Hz, with constant strain amplitude of 30 μm. A static pre-load of 1N was applied before the tests to keep the sample tight. Three samples were tested under each of the studied conditions.

2.2.3. Biological evaluation

For these experiments membrane samples of 1 cm^2 were obtained and the behaviour of L929 mouse lung fibroblasts on passage 31 and human immortalized Schwann cells on passage 20 were studied. These cells were seeded separately in 24-well cell culture plates, at a density of 3000 cells/cm^2 for metabolic activity assay and 6000 cells/cm^2 for proliferation assay, due to the different sensibility of each kit. L929 fibroblasts were incubated with Low Glucose DMEM medium, supplemented with 10% FBS and 1% penicillin/streptomycin, at 37 °C in 5% CO_2. Immortalized Schwann cells were cultured under the same conditions, but the culture medium was High Glucose DMEM and was also supplemented with 1% Sodium Pyruvate. In all the following experiments, samples were appropriately washed with PBS and correspondingly analyzed after 1, 3 and 7 days in culture.

2.2.3.1. Live/dead viability assay

The viability of L929 fibroblasts and immortalized Schwann cells seeded over the studied membranes was evaluated using Calcein AM and propidium iodide staining. After 1, 3 and 7 days of culture, each seeded membranes was washed with PBS and immersed in 1 mL of culture medium supplemented with 1 μg Calcein AM and 2 μg propidium iodide. These immersions lasted for 15 min, after which the samples were washed with PBS and analyzed using a transmitted and reflected light microscope (Axio Imager Z1m, Zeiss, Jena, Germany).

2.2.3.2. Metabolic activity quantification in 2D cultures

L929 fibroblasts and immortalized Schwann cells metabolic activity was followed with Alamar Blue (AB), a dye that yields a fluorescent signal and a colorimetric change when incubated with metabolically-active cells. Cell culture medium containing 10% AB was added to the different culture wells and the systems were left for incubation during 3 h, after which 100 μL of each solution were trans-

UNCORRECTED PROOF

ferred to white opaque 96-well plates, in triplicates. Fluorescence was monitored at 590 nm emission wavelength (excitation wavelength 530 nm), using a microplate reader (FL 600, Bio-Tek Instruments). PBS was used for removing the AB reagent and fresh medium was added in its place after each AB determination. The metabolic activity values were calculated by normalization with the mean fluorescence value obtained for the controls (Tissue culture polystyrene; TCPs) with and without cells.

2.2.3.3. Cell proliferation quantification in 2D cultures

In order to assess L929 fibroblasts and immortalized Schwann cells proliferation CyQUANT® Cell Proliferation Assay Kit was used. After 1, 3 and 7 days the culture medium was removed from the wells, the samples were washed with PBS, placed in new wells and culture medium incorporating 0.4% of CyQUANT® Direct nucleic acid stain and 2% of CyQUANT® Direct background suppressor was added to the wells. The samples were incubated for 2 h at 37 °C, in 5% CO_2 atmosphere. The fluorescence intensity of each sample was measured using a fluorescence microplate reader (FL 600, Bio-Tek Instruments). The excitation wavelength was 485 nm and the emission detection was performed at 528 nm. All measurements were done in triplicate and the number of cells present in the different samples was calculated by using a calibration curve.

2.2.3.4. Cells morphology and cytoskeletal organization

For determining the morphology and cytoskeletal organization of L929 fibroblasts and immortalized Schwann cells DAPI (4,6-diamidino-2-phenylindole-dilactate fluorescent dye)-phalloidin (phalloidin tetramethylrhodamine B isothiocyanate fluorescent dye) assay was performed.

At each timepoint (1, 3 and 7 days of culture) the corresponding samples were washed with PBS after culture media removal and fixed in 10% formalin during 1 h. Afterwards, formalin was removed by PBS washing and 1 mL of PBS containing 2 μL of phalloidin (10 mg/mL) was added to the systems, leaving them to react for 40 min at RT. After extensively washing with PBS, 1 mL of PBS containing 1 μL of DAPI (20 mg/mL) was incorporated to the systems and left to react for 10 min. The dye was removed by washing with PBS. Finally, the samples were analyzed using a transmitted and reflected light microscope (Axio Imager Z1m, Zeiss, Jena, Germany).

2.3. Statistical analysis

All the performed tests were conducted in triplicate and the obtained data points are presented as mean ± standard deviation. The statistical results in the biological characterization were analyzed using GraphPad Prism software. One-way analysis of variance (ANOVA) was used to establish statistical differences between the different materials (n = 6). $P < 0.05$ was considered statistically significant.

3. Results

3.1. Physicochemical and surface characterization of membranes

Three types of chitosan membranes, differing on the degree of acetylation (DA I: 1%, DA II: 2% and DA III: 5%), were produced and analyzed (Table 1). All of them were almost transparent, with DA I and DA II having average thickness of 30 μm, while DA III was around 100 μm thick.

3.1.1. SEM micrographs

SEM pictures (Fig. 1A) show very smooth and flat surfaces for the three samples.

3.1.2. AFM

It was determined that the mean roughness (Ra) in dry state was 6.3 ± 0.48 nm, 3.7 ± 0.82 nm and 7.2 ± 0.24 nm and after two hours in PBS the mean roughness was 7.3 ± 0.043 nm, 5.1 ± 0.64 nm and 7.5 ± 0.35 nm, for DA I, DA II and DA III membranes, respectively (Table 1). Representative micrographs of membranes in simulated physiological conditions can be seen in Fig. 1B (AFM micrographs of the dry membranes are not shown). DA II film has a smoother surface, indicated by the lowest mean value of Ra, when compared to DA I and DA III.

3.1.3. Contact angle and surface energy

The water contact angles and the calculated surface energy for the three chitosan membranes can be seen in Table 1. Water contact angles are 107.1° ± 0.33, 95.6° ± 4.49 and 115.2° ± 1.96 for DA I, DA II and DA III, respectively. Regarding surface energy, values of 32.07 ± 0.00 mN m^{-1} (DA I), 31.53 ± 0.01 mN m^{-1} (DA II) and 35.22 ± 0.01 mN m^{-1} (DA III) were obtained.

3.1.4. FTIR

FTIR spectroscopy can be seen in Fig. 2A. As expected, the transmission infrared spectra of all chitosan membranes exhibited a broad peak in a range from 3450 to 3390 cm^{-1}, assigned to OH stretching, representing intermolecular hydrogen bonding of chitosan molecules. In the same region, a peak corresponding to N—H stretching would also be visible, but it is overlapped with that of the OH stretching. The more acetylated form of the membranes (DA III) has a new peak at 1655 cm^{-1}, related to secondary amides. This peak is not visible in the two less acetylated membranes. On the other hand, DA I and DA II membranes display one peak at 1596 cm^{-1}, relative to N—H deformation. This means that during the *N*-deacetylation that took place for the obtaining of chitosan, the band at 1655 cm^{-1} gradually decreased, while that at 1590 cm^{-1} increased, thus indicating the prevalence of NH_2 groups.

3.1.5. XRD

After all the processing, only a diffuse peak is visible near 20° (2 Teta) (Fig. 2B), indicating that the studied chitosan samples lost their crystallinity and remain in an amorphous state.

3.1.6. DSC

There were no differences in the DSC thermograms regardless of their DA. A broad endothermic peak appearing during the first heating cycle is attributable to water evaporation at approximately 80–110 °C (data not shown). The second heating spectra (Fig. 2C) revealed that all chitosan membranes have mainly one reaction zone, represented by an exothermic peak, which is related to the decomposition of the polymer (onset at 250–300 °C). In our studies, it was not detected the presence of any glass transition.

3.1.7. Weight loss and water uptake

The results of weight loss and water uptake can be seen in Fig. 3. After PBS immersion there was a weight loss of around 4% after 30 days for all the membranes (Fig. 3A), indicating negligible hydrolysis phenomena. The membranes immersion in PBS with 13 mg/L of lysozyme also reveals reduced weight loss for all the membranes (Fig. 3B), indicating minor enzymatic degradation. To visually evaluate the degradation of the chitosan membranes in the presence of lysozyme, SEM micrographs of degraded membranes (DA I, DA II and DA III) can be seen in Fig. 4B, in comparison with the original aspect of dry membranes (Fig. 4A). Differences in the surface morphology can be clearly appreciated, since it is visible the flat and smooth aspect of the original membranes, in contrast to the wrinkled

UNCORRECTED PROOF

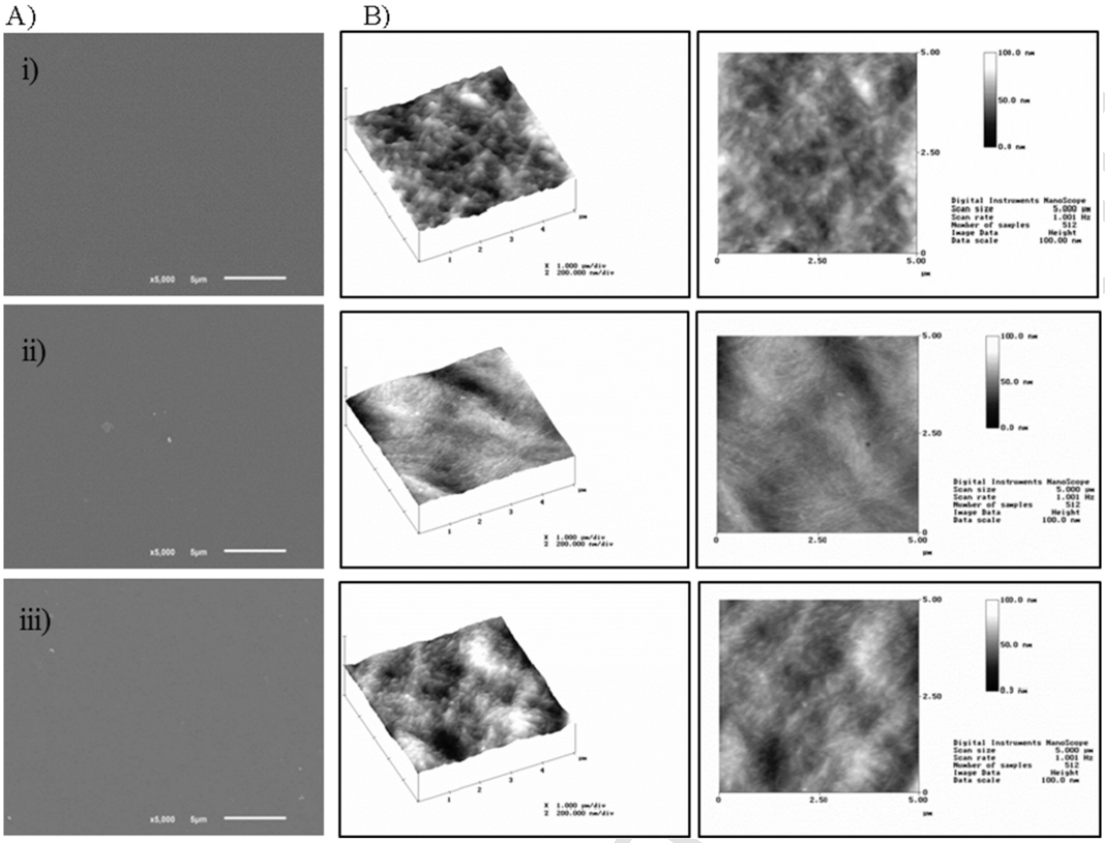

Fig. 1. Surface characterization of chitosan membranes (i – DA I; ii – DA II; iii – DA III). A) Scanning Electron Microscopy micrographs. Scale bar 5 μm; magnification 5000 ×; B) Atomic Force Microscope three dimensional images of chitosan membranes under simulated physiological conditions by previous 2 h immersion of samples in PBS. 5 μm × 5 μm scan area; contact mode.

and rough features in the surface of the lysozyme treated ones. Thus, despite in terms of weight loss percentage there are not stand out variations, the degrading effects of the lysozyme can be appreciated in all chitosan membranes, regardless of the DA.

Regarding the water uptake (Fig. 3C), the studied membranes absorbed water progressively during one day, losing some of this gained weight during the following 15 days, to finally reach a stabilization in the water content between 15 and 30 days. In this last period the swelling was near 40% of the membranes original weight for DA I and DA II and 50% for DA III. All along the time of the study (30 days) the membrane with the higher DA (DA III) showed greater water uptake capability than those with the lower DA (DA I and DA II).

3.1.8. Bioactivity

For all the studied samples, SEM images (Fig. 5) revealed crystal or apatite free membranes after 1, 15 and 30 days of immersion in SBF (see the examples of the first and last timepoints evaluated, 1 and 30 days). The absence of peaks corresponding to Ca and P ions after EDS analysis confirmed these previous results.

3.1.9. Mechanical properties

The mechanical analysis results are presented in Fig. 2D. Comparing the membranes DA I and DA II the difference between the modulus (E′) are almost imperceptible. However, for the higher degree of acetylation studied (DA III), a slight decrease of storage modulus (E′) can be observed. It was found that for all the studied membranes, E′ did not suffer variations with increasing frequency. The second graph shows the frequency influence on the loss factor (tan δ). Values of tan δ between 0.15 and 0.2 were obtained for all the three membranes, all along the contemplated frequency range. As in the previous case, tan δ values for DA I and DA II membranes were quite similar, while membrane DA III presented modest difference with respect to them, having slightly lower tan δ values.

3.2. Biological characterization

In the live/dead assay of L929 fibroblasts very few green cells can be observed, regardless of the timepoint or DA (Fig. 6A). Concerning the SCs (Fig. 6B), spread green cells can be seen, their number increasing with time and with the degree of acetylation of the CHT in the membranes.

Fig. 7A and B shows the metabolic activity of L929 fibroblasts and Schwann cells, respectively, determined by means of AB analysis. At all timepoints considered, the relative fluorescence units (RFU) corresponding to L929 fibroblasts were under 100 for all three membranes, diminishing with time from the first timepoint studied. On the contrary, in the case of the SCs, the RFU values increased progressively along the time of the study, being this tendency more pronounced in the case of the film with the higher degree of acetylation (DA III). For this cell line RFU values were between 50 and 100 in the case of DA I and DA II membranes, which showed a marked difference with membrane DA III, which showed an increase from 50 RFU in the first timepoint (1 day) to 400 RFU in the seventh day of the study. These results were supported by cell proliferation analysis, showing values around 19 RFU for L929 fibroblasts at the seventh day of study (Fig. 7C), while in the case of the SC they were near 26 RFU (Fig. 7D) at that same timepoint.

UNCORRECTED PROOF

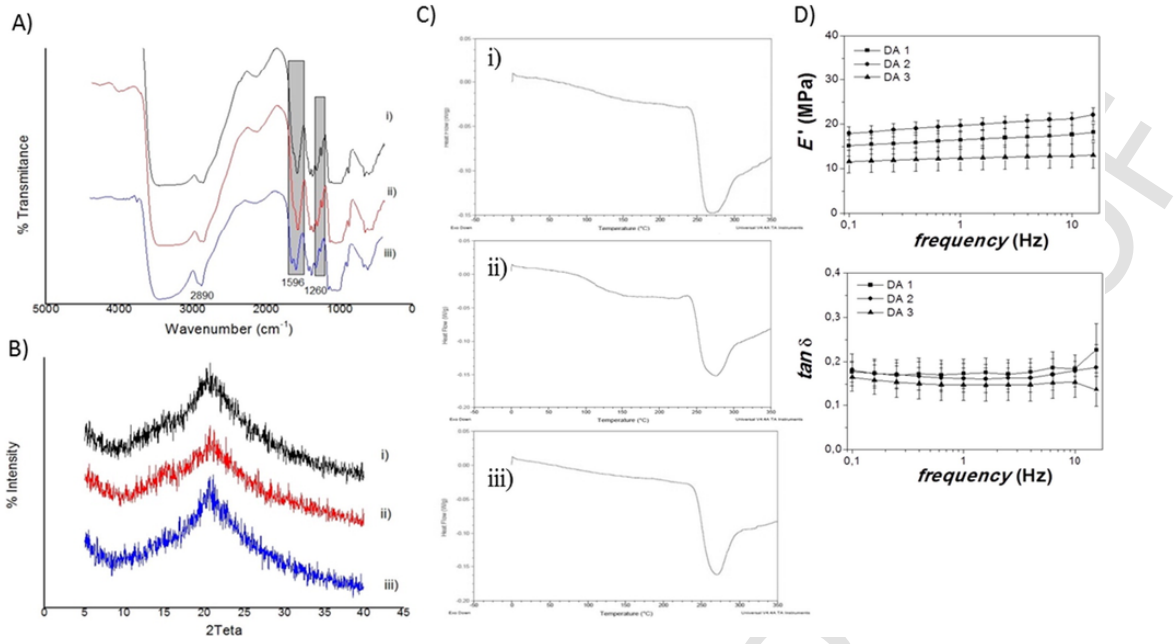

Fig. 2. Physicochemical characterization of chitosan membranes (i – DA I; ii – DA II; iii – DA III). A) Fourier Transforming Infrared Spectroscopy analysis. 32 scans with resolution of 4 cm^{-1}, corresponding to the 4000–400 cm^{-1} spectra region. B) X-ray diffraction patterns of the studied chitosan membranes. Fixed incidence angle of 1° between the incident X-rays and specimen plane. C) Differential Scanning Calorimetry thermograms of chitosan membranes. Second heating cycle, ranging from 0 °C to 350 °C at a rate of 1 °C/min. D) Mechanical properties analysis of chitosan membranes. Storage modulus (E′) and loss factor (tan δ) of the three studied chitosan membranes measured as a function of frequency. Studies performed at room temperature.

Phalloidin/DAPI staining proves that L929 cells (Fig. 8A) present a round, non- typical fibroblasts morphology, clearly indicating a lack of adhesion of these cells to the membranes. Nevertheless, after SCs phalloidin/DAPI staining (Fig. 8B) a characteristic spindle shaped and elongated morphology of the cells can be clearly appreciated, thus proving their good adhesion to the studied systems.

4. Discussion

Chitosan has been described as an interesting biomaterial to be used in peripheral nerve engineering, as it promotes cells adhesion and proliferation [17,26,36,37]. Chitosan with a wide range of degrees of acetylation has been tested before for several regenerative applications. The results indicate that regardless of the cell type, the general rule is that lower DA chitosans promote higher cell adhesion [20,25,26,29–33]. However, the gaps between the analyzed DA values are relatively large and in most cases, while the lowest DA value analyzed is essentially from 1% to 10%. For instance, Chatelet et al., [25] evaluated a range of DA varying from 2.5% to 47% and the lowest presented the best cell adhesion results. Also, Freier et al. [26], studied a range that went from 0.5% to 99%, also concluding that the lowest DA % presented the best biological outcome. However, in this work, the authors did not perform an extensive physicochemical characterization. In a third study Amaral et al. [31], undoubtedly disclosed that for a range of DA varying from 4.23% to 49.1%, the lowest presented the most promising results for bone regeneration. Considering these particular results, we believe that values from 0% to 5% acetylated would be the most suited for tissue engineering and regeneration and worth studying in detail.

Therefore, in the present investigation, chitosan powders with three different low DAs (DA I: 1%, DA II: 2%, DA III: 5%) were employed in the production of membranes for peripheral nerve regeneration purposes. The differences at a physicochemical and biological level among the different membranes were examined, with the ultimate objective to discern which one of them will be the most appropriate for its application in peripheral nerve regeneration.

In any scaffold to be implanted, the role played by the surface morphology and topography is a major parameter influencing cell adhesion and proliferation, and, eventually, the scaffold rejection or acceptance [38].

SEM and AFM characterization showed very smooth and flat surfaces for all the studied membranes, with higher roughness for more elevated DA values. This is in concordance with the literature, where it is described that the parameter increases with the DA, due to an increment of acetyl groups, which will originate the formation of fibrillary aggregates. The increase in molecular weight as the DA does have also been related to roughness increments [31].

During the SEM and AFM characterization it was observed that the membrane DA II did not follow the expected tendency. Consequently, it was postulated that preparation and processing procedures should gave rise to some sort of unexpected superficial modification. This premise should be confirmed after further analysis of the membranes surface.

Non-covalent forces established between liquids and the first monolayer belonging to the studied materials can be measured by contact angle. It is well-known that a smaller water contact angle is linked to better surface wettability, which will ultimately be more favourable for cell adhesion than a hydrophobic surface [31,39].

The water contact angle of DA III is higher with respect to that of DA I, which is within the expected, as it has been stated that contact angle changes with the DA, following a direct proportion. Also as expected, an inverse tendency is observed regarding the wettability. One possible reason for this is that the lower the DA, the more free amine functionalities at the surface. These amino groups may become protonated at neutral pH, resulting in a high positive surface charge that promotes the ability of the membranes to interact with water [40,41].

The obtained results related to surface energy (SE) proved the Dispersive component as the main parameter contributing to the sur-

UNCORRECTED PROOF

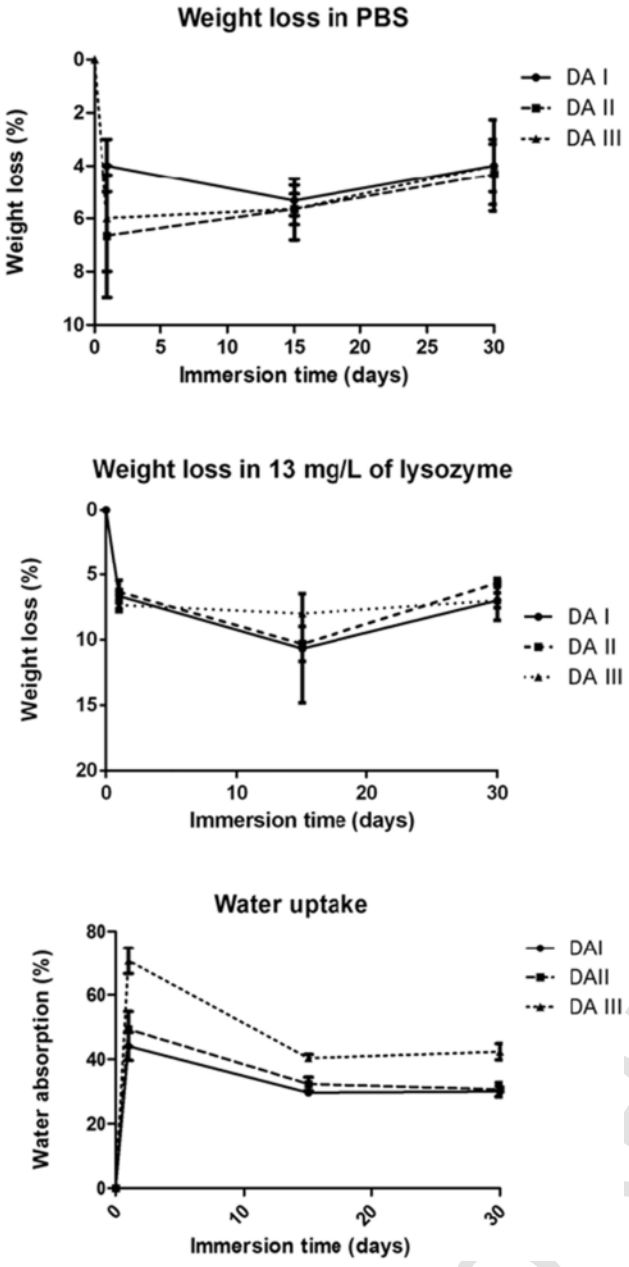

Fig. 3. Weight loss and water uptake of chitosan membranes at 37 °C for different time periods; A) weight loss of studied chitosan membrane formulations after storage in PBS; B) weight loss of studied chitosan membrane formulations after storage in PBS with 13 mg/L of lysozyme; C) water uptake of samples after storage in PBS. The data represents the mean for each timepoint ± standard deviation.

face energy, consequently showing a slight increase in the SE for DA III, with respect to DA I. These results are in concordance with what has been said in the preceding paragraphs. As it has been postulated before [42], higher surface energy enhances cell adhesion in the early stage of cell response, possibly inducing the expression of adhesion-associated molecules.

The previous surface analyses confirm the existence of some sort of superficial abnormality for DA II membrane, possible consequence of its production/processing.

FTIR spectroscopy was used to obtain information about the molecular state and bulk properties of chitosan membranes. The results showed the typical spectra usually obtained for low acetylated chitosans, where some of the typical glucosamine peaks were identified. The spectra corresponding to the three studied membranes were very similar between them, as expected, due to the similar DAs of the raw chitosans. Indeed, more distant DAs would give rise to more noticeable variations in the FTIR spectra, particularly, the band associated with the vibration of C ═O bond from secondary amide (amide I), barely observed on DA III membrane, but clearly described in other works [30,43]. These spectra made also possible to confirm that no contamination or any other kind of impurities were present in our formulations.

XRD analyses were carried out to determine the structural nature of the studied formulations, more specifically, whether the membranes are amorphous or crystalline. Up to date, there are contradictory results regarding this parameter, as some authors [30,44] found that the lower the DA, the higher the degree of crystallinity. However, others [45,46] observed that the crystallinity decreased with the decrease in DA. What is clear is that besides by the DA, the crystallinity of chitosan membranes can be also highly influenced by the source of the material, the preparation or dissolving conditions and the drying procedure [47]. Indeed, in the case of the membranes analyzed in this experimental work, no structural differences were found as a function of the DA, as all formulations were in an amorphous state, proved by the presence of a diffuse XRD peak near 20° (2 Teta) and the absence of two intense peaks at 10° and 20° [48]. These results are in concordance with the literature, were it is described for chitosan membranes prepared by the solvent-casting technique, starting from an aqueous acetic acid solution, to be in an amorphous state. This may be caused by residues of the acetic acid solvent, which may impede the creation of inter and intramolecular hydrogen bonds between chitosan chains, resulting in a more irregular structural organization and thus a distancing from crystallinity [28,49].

Differential Scanning Calorimetry is a powerful technique for studying the thermodynamics of polymers. It can provide a basic understanding of its behaviour with different temperatures. In a first heating cycle where temperature was raised to 200 °C, an endothermic peak corresponding to water evaporation appears in the obtained thermograms (data not shown). This evaporation was performed to avoid the water present in the chitosan membranes (chitosan is prone to absorb moisture) to act as a plasticizer, lowering the Tg (Glass Transition) temperature and giving rise to erroneous results [50]. The second heating cycle of the experiment (0–350 °C) proved that there is no glass transition for the studied chitosan membranes. These materials do not melt, but degrade at elevated temperatures, as indicated by the exothermic peak near 300 °C present in all the thermograms [51].

Degradation is an important parameter to take into account when the use of a scaffold for peripheral nerve regeneration is envisioned. The ideal device should remain intact during axon regeneration, and then progressively degrade [52]. In this experimental work the degradation will be referred to as weight loss (WL).

Weight loss of the membranes in PBS was negligible, proving that they were stable in aqueous solutions at a physiological pH during the period of study (30 days) and did not suffer significant hydrolysis. In addition, weight loss studies were also performed in PBS containing the enzyme lysozyme, the principal endogen enzyme responsible for chitosan degradation. Lysozyme transforms chitosans from high molecular weight polymers to oligomers, and it is found in various human body fluids and tissues, including serum and tears [53]. It should be pointed out that no accelerating conditions, as low pH or high enzyme concentrations, were used.

The WL values obtained were similar to the ones obtained in the absence of the enzyme. The lack of consecutive *N*-acetyl-D-glucosamine residues in low DA materials is responsible for the poor chain cleavage of chitosan, because their degradation kinetics are in-

UNCORRECTED PROOF

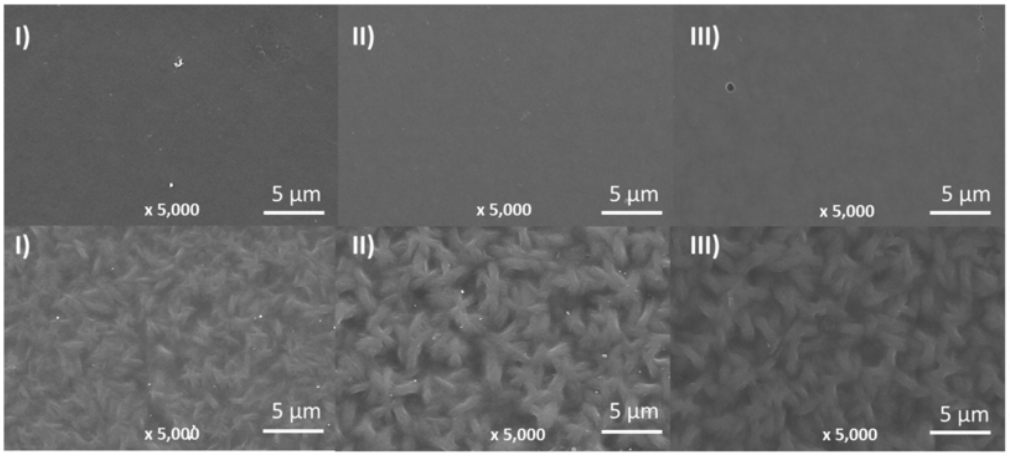

Fig. 4. Scanning Electron Microscopy micrographs of chitosan membranes (i – DA I; ii – DA II; iii – DA III). A) Micrographs of dry unmodified surface; and B) micrographs of dry membranes after 30 days in PBS in the presence of 13 mg/L of lysozyme. Scale bar corresponds to 5 µm.

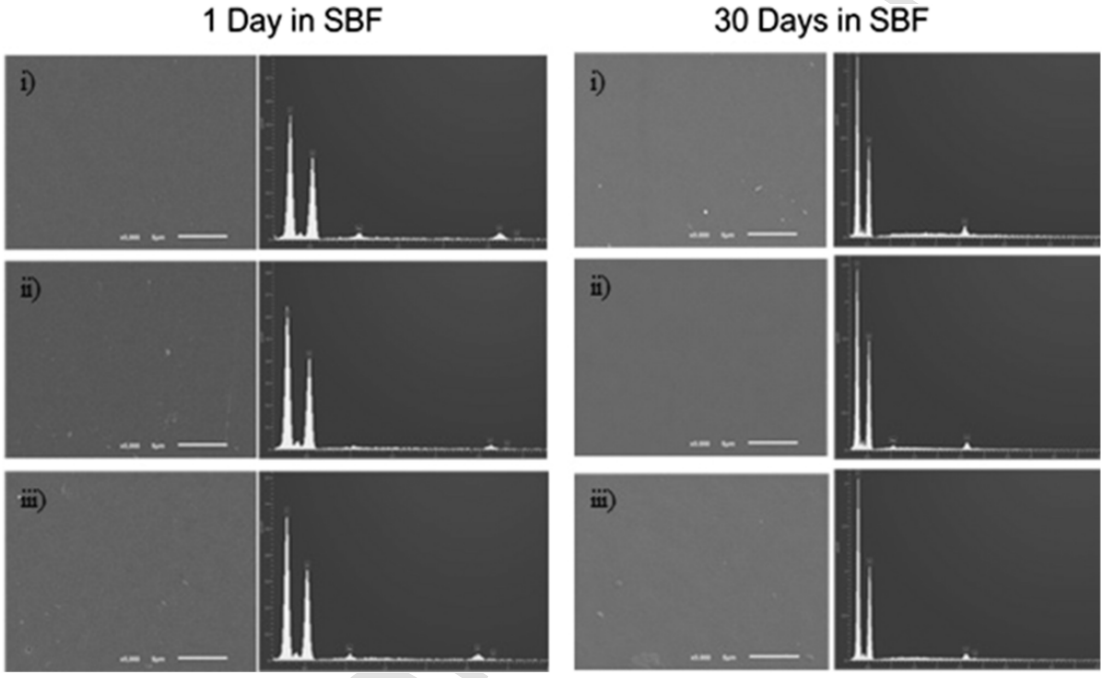

Fig. 5. Scanning Electron Microscopy and EDS analysis of chitosan membranes after 1 and 30 days in SBF: A) DA I after 1 day in SBF; B) DA II after 1 day in SBF; C) DA III after 1 day in SBF; D) DA I after 30 days in SBF; E) DA II after 30 days in SBF; and F) DA III after 30 days in SBF. Scale bar 5 µm; magnification 5000 ×.

versely related to the degree of acetylation. This can be explained by the fact that molecules consisting primarily of β-1,4-linked D-glucosamine residues are not accessible to the lysozyme active site. Indeed, the lysozyme can only access and act on sites where more than three *N*-acetyl-D-glucosamine sequences are present.

A more extensive explanation for this phenomenon can be found elsewhere [26,53].

One of the key aspects influencing the effectiveness of chitosan conduits in nerve repair is the swelling ability. It is critical to guarantee that swelling will not cause compression phenomena in the implanted scaffold, pressing the nerve or occluding the lumen, which could lead to ineffective nerve functioning and regeneration [6]. Still, it is important that the material swells to a certain extent *in vitro*, to be able to integrate the culture medium needed for cell survival, and *in vivo*, to mimic endogenous tissues, which are mainly composed by water (≈ 60% of the total weight). In this experimental work the swelling will be referred to as water uptake (WU).

Chemically, the swelling performance of a material is a balance between the presence of hydrophilic groups able to interact with water and the amount and strength of intramolecular bonds. Despite having the lower surface wettability, the membrane DA III is the one having the higher water uptake (inversely to what occur for the membrane DA I). This is attributed to the fact that intramolecular hydrogen bonds established between hydroxyl groups and amino groups are stronger than that formed between these same groups and water molecules [44]. The bonding strength can result in more rigid structures, unable to efficiently incorporate, or even prone to extrude water. The membranes composed by the chitosans with the higher degrees of acetylation have less amine groups available, with respect to the ones with the lowest DA, thus favouring the entering of water.

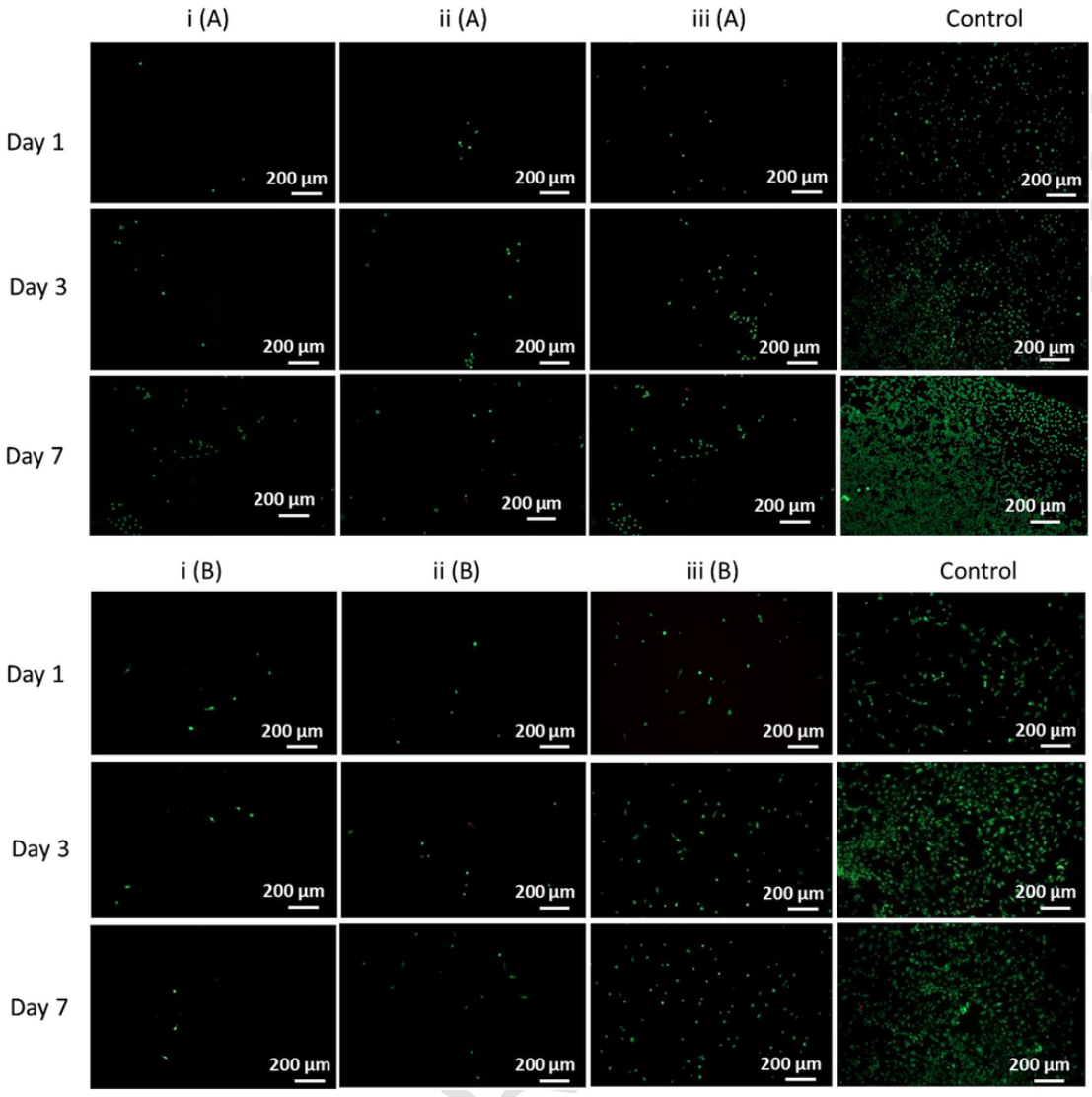

Fig. 6. Viability live/dead assay of cell lines after 1, 3 and 7 days after direct seeding on chitosan membranes. Live cells stained with Calcein (green color) and dead cells stained with propidium iodide (red color). A) L929 cell line viability on chitosan films; and B) Schwann cell line viability on chitosan films. Scale bar corresponds to 200 µm. (For interpretation of the references to color in this figure legend, the reader is referred to the web version of this article.)

In vitro biomineralization of the produced membranes would be an undesired phenomenon for peripheral nerve regeneration applications, since the appearance of calcification around the implanted material will have negative effects over the regenerative process. Although chitosan itself usually does not have the capacity to calcify, it should be assured that our membranes would not mineralize under conditions similar to human body. Since no traces of Ca and P were detected in the surface of the membranes after 30 days in SBF, it can be asserted that no mineralization occurred.

When speaking about implanted materials it is important to take into account that, to a higher or lower extent, they will have to withstand mechanical stress. Indeed, a nerve is under tensile load *in situ*, as evidenced by the fact that it retracts when severed. The biological mechanical parameters of tissues comprehend a wide spectrum of values. In the specific case of artificial nerve grafts, they will have to endure the *in situ* stress to which peripheral nerves are submitted, while suture holding ability will also be needed. In addition, it is well-known that cells have a specific behaviour in response to mechanical stress. The structural organization of peripheral nerves enables them to function while tolerating and adapting to stresses placed upon them by postures and movements of the trunk, head and limbs. They are exposed to combinations of tensile, shear, and compressive stresses that result in nerve excursion, strain and transverse contraction. Thus, the tolerance of nerve guidance conduits to stiffness and strength should be enough to cope with the *in vivo* developed stresses, without collapsing or losing shape. For this reason, a proper mechanical characterization makes part of the most important physical tests to be performed over an implantable PNR system [54,55].

Dynamic mechanical analysis (DMA) is a non-destructive technique that permits to characterize the mechanical and viscoelastic features of biomaterials, given an idea about which will be their mechanical behaviour after *in vivo* implantation [56]. Taken into account the high moisture conditions of the physiological environment, it is expected for the membranes to be hydrated once implanted in the human body, and for this reason they were immersed in PBS before the DMA measurements.

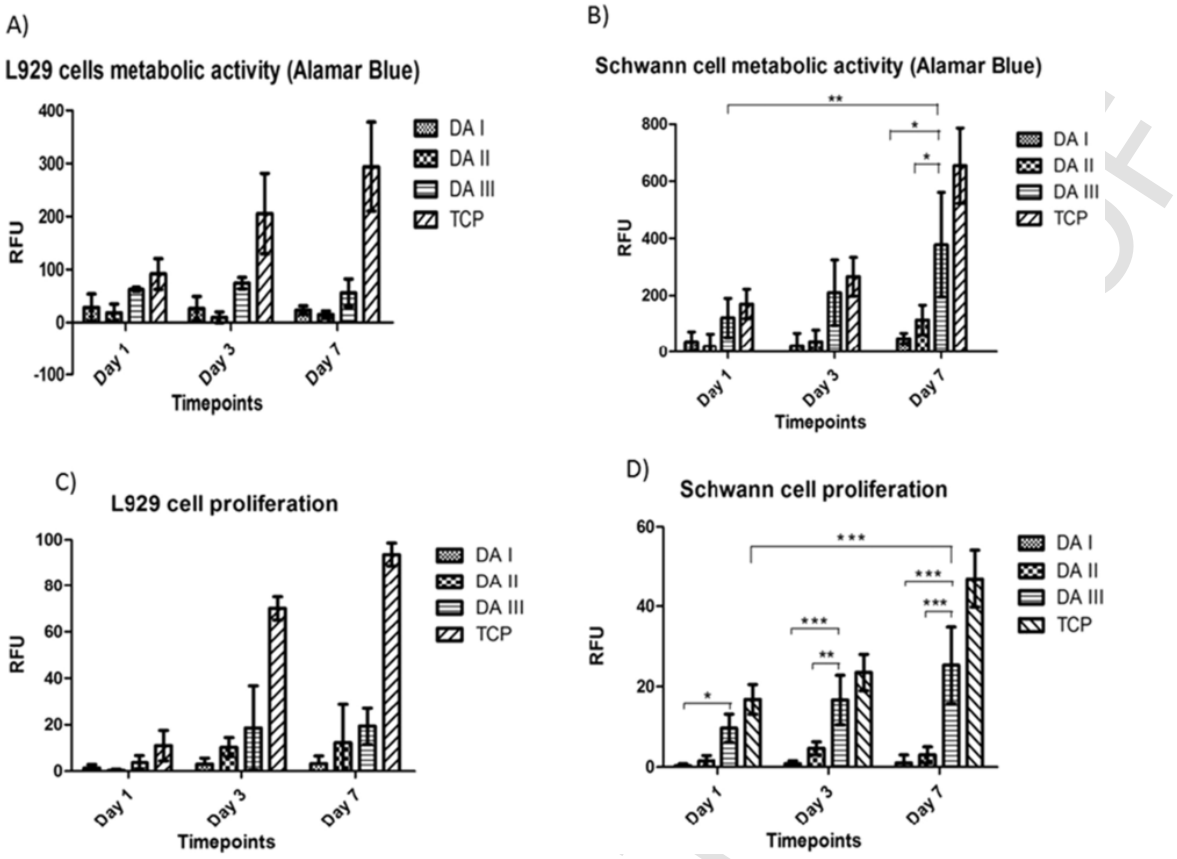

Fig. 7. *In vitro* cell culture studies: A) metabolic activity of L929 cells seeded on chitosan films determined by Alamar Blue after 1, 3 and 7 days; B) metabolic activity of Schwann cells seeded on chitosan films determined by Alamar Blue after 1, 3 and 7 days; C) proliferation of L929 cells seeded on chitosan films determined by CyQUANT® Cell Proliferation Assay Kit after 1, 3 and 7 days; and D) proliferation of Schwann cells seeded on chitosan films determined by CyQUANT® Cell Proliferation Assay Kit after 1, 3 and 7 days.

The membranes DA I and DA II have a similar E′. However, a more pronounced difference is observed for DA III, presenting the lower E′, which is synonymous of a lower stiffness. An occurrence of a slight decrease of storage modulus (E′), and also loss factor (tan δ), with the increase in the DA is confirmed by literature [30].

This behaviour is consistent with the water uptake ability of the membranes and the plasticization effect of water molecules in such kind of polysaccharides, increasing their molecular mobility and decreasing the stiffness of the material. A similar loss of the stiffness due to the effect of water interacting with chitosan molecules was previously reported in pure chitosan membranes [57]. It should also be pointed out that in all the membrane formulations no evident variations of E′ along the frequency axis were seen, indicating that no relaxation phenomena took place in the membranes within the time scale covered by the experiments, and confirming their structural stability along the studied frequency range. The tan δ provides information about the damping properties of the material [58,59]. In this case, DA III was the membrane with the lower tan δ, indicating a higher elastic character.

In a general manner, the developed membranes presented ≈ 10 to 20 MPa in Young Modulus, allowing the cell attachment and spreading, favouring Schwann cell proliferation when compared to L929 fibroblasts. As expected and previously reported in the literature, in a general way, nervous system cells prefer softer and more flexible membranes [60–62], which was the case of DA III, with ≈ 10 MPa in Young Modulus. The values of healthy peripheral nerves vary greatly in the literature. Related to fresh healthy nerves, the values of Young Modulus in mice and rats are very low [63] when compared to pigs [64] creating a range that goes from 0.5 MPa (in mice) to 7.75 MPa (in pigs). In this respect, comparing our data with the values of mechanical properties to fresh healthy *in vivo* nerves in pigs [64,65] the values were similar and in the same range of the ones reported in the literature for porcine peroneal and tibial nerves (≈ 7.43–7.75 MPa).

Although it is a general concept in tissue engineering that mechanical strength of nerve guidance conduits should not outperform the peripheral nerve mechanical properties [6], there is a large variability in mechanical properties of biomaterials envisioned for peripheral nerve regeneration. Indeed, little research has been performed to find the standard reference value for ideal materials to be used with this goal.

Hydrogels normally present a low value of Young Modulus, up to 1 MPa [66–68].

Fabricated membranes planned for peripheral nerve regeneration usually show higher values of Young Modulus. For instance, PCL/PLA films revealed values ranging from 60 MPa in one study [69] to 175.52 in other report [70]. When we consider poly-ε-caprolactone membranes, they have Young Modulus values ranging from 108.90 ± 7.13 to 69.60 ± 13.83 [71]. All the references cited above display much higher values than the ones presented by the studied low acetylated chitosan membranes (≈ 10 to 19 MPa). These results were also compared to other values obtained for chitosan membranes, with similar conclusions [30].

After damage in peripheral nerves, a series of physiological events take place, named Wallerian degeneration. As part of the process, Schwann cells dedifferentiate and proliferate to participate in the removal of myelin and axon debris, to secrete a series for neurotrophic factors and to form the bands of Bungner, which will act as guide for the regenerating axons. Ultimately, Schwann cells (SCs) will help in

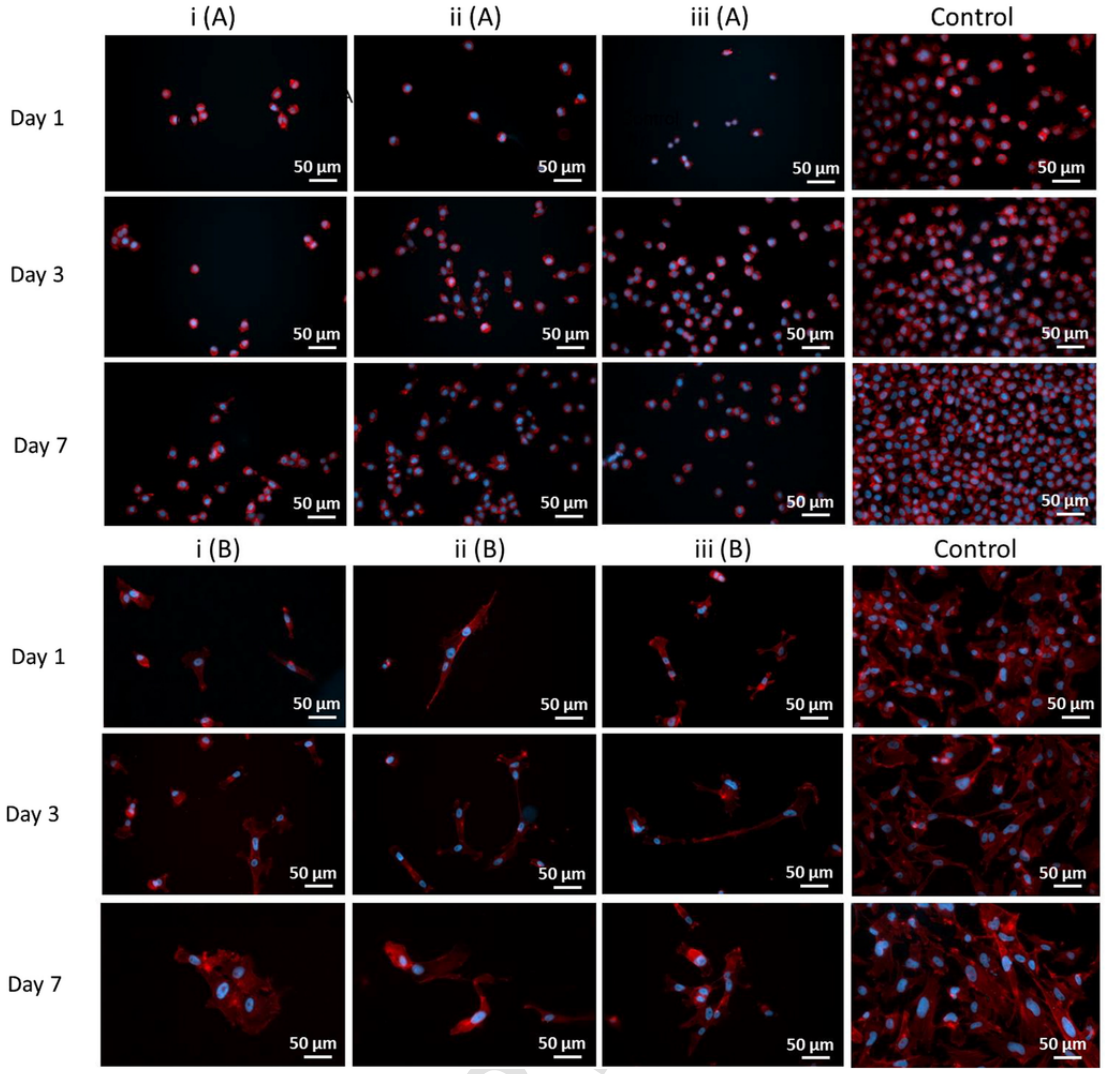

Fig. 8. Phalloidin/DAPI staining of cell lines after 1 (i), 3 (ii) and 7 (iii) days after direct seeding on chitosan membranes. A) L929 cell line morphology on chitosan films; and B) Schwann cell line morphology on chitosan films. Scale bar corresponds to 50 μm.

axon re-myelinization. Consequently, for an implant to mediate a successful guided regeneration, it should promote SCs adhesion and proliferation [72]. Simultaneously, the formation of fibrotic tissue is started. This process has the purpose to avoid the extension of the damage, but supposes one of the main causes of regeneration failure. This appearance of fibrotic tissue is mediated by excessive fibroblasts infiltration and excessive collagen production [73,74]. Fibroblasts are the primary cell type participating in collagen synthesis and the build-up of connective tissue, as these cells are responsible for normal tissue homeostatic processes, such as tissue repair in response to injury. For this reason, the obtaining of a PNR scaffold able to avoid excessive fibroblast adherence will be of fundamental importance, although it is a clear technological challenge.

At the seventh day of the study the control of fibroblasts showed a much higher number of cells when compared to that corresponding to SCs. Nevertheless, the high proliferation of fibroblasts in the controls contrasts with the one in the membranes, thus indicating an inefficient capacity of these systems to support fibroblasts growth. Regarding SCs, the ability of the studied formulations to support the proliferation of this cell line was evidenced, with a much positive outcome in the case of DA III.

The results obtained for L929 fibroblasts proved a low metabolic activity of the cells seeded in the DA membranes when compared to the controls. In the case of SCs, clearly smaller differences can be appreciated between the controls and the studied formulations. The DA III membranes were the ones giving rise to higher metabolic activity values, with significant differences regarding DA I and DA II and the initial and final time-points of study.

The proliferation of fibroblasts in the three membranes was much lower than in the controls, while the formulation inducing higher proliferation of SCs was the DA III, with significant differences with respect to DA I and DA II. Although the value of RFU for Schwann cells also seem low, it should be kept in mind that this specific cell line presents low values of RFU when submitted to this type of studies. In accordance, these results confirmed the ones obtained in the cell metabolic activity studies.

In the case of L929 cells, phalloidin/DAPI revealed that these cells are not expressing their habitual phenotype, an indicative of the absence of adherence to the membranes. Nevertheless, SCs seeded in the DA III membranes presented their characteristic functional phenotype, spread and elongated.

The biological tests also confirmed a much better adherence and proliferation of SCs, including typical phenotypic differentiation,

than fibroblasts to the analyzed membranes, above all noticeable in the case of the DA III one.

One possible explanation for that is related to the mechanical properties. Cells are known to apply tension on their substrate, particularly during adhesion and migration processes, and have the ability to sense the underlying elasticity through their cellular receptors, primarily integrins, which then act as mechanotransducers. Well-described mechanotransducers include stretch-mediated ion channels [75], primary cilia [76] and integrins [77]. Stiffness sensing has been demonstrated in a variety of cell types including endothelial cells [78], smooth muscle cells [79] transformed cells [80] and, specifically relate to PNR, Schwann cells [62] and fibroblasts [81].

Fibroblasts are known to have a superior adhesion in rigid substrates, and this apparent preference for a stiff substrates is known as "durotaxis" [81].

On the other hand, nervous system cells and components such as Schwann cells and neurons, have a preference for softer matrix [60–62]. Therefore, mechanics are an essential parameter for regenerative medicine and have to be controlled in detail, so they can influence specific cell adhesion. In relation to the studied samples, the native mechanical environment of DA III membrane was able to elicit a favourable Schwann cell response, since it presented itself as less stiff and more elastic, when compared to DA I and DA II.

This not only explains why Schwann cells adhere in a higher extent to this matrix when compared to fibroblasts, but also sheds light on why DA III membrane was remarkably better in relation to less acetylated membranes.

This modulated and preferential cellular adhesion is a good preliminary indicator for potential SC colonization and low fibroblastic infiltration once the systems are implanted *in vivo*. It is important to take into account though, that the presence of a certain amount of fibroblasts will be necessary to sustain the healing process.

Another possible explanation is an interaction based on non-specific electrostatic forces occurring between protonated amine groups from glucosamine units and negatively charged carboxylate and sulphate groups found onto the specific cell surface [31].

DA III revealed itself as the membrane with higher potential for PNR purposes, thus being the one selected for further studies.

Although the general conclusion from most studies is that the lowest DA value possible is normally the best in terms of cell adhesion, our findings were different after the extensive characterization of these membranes, having the best result for the 5% DA membrane. However, our results are in agreement with another report focused on chitosan targeted for PNR, in which the optimal DA was also 5% [16]. The physicochemical characterization played a crucial role in the understanding of the obtained results, also shedding light on how and why such particular biological performance was displayed. To the superior performance of DA III membrane contributed its increased roughness and surface energy as well as adequate mechanical properties.

We fundamentally studied in detail this niche of low DA values for tissue regeneration and effectively found significant differences between them, which was our initial hypothesis.

The physicochemical and biological features of DA III membrane, revealed it as a very versatile and promising biomaterial to be explored in peripheral nerve regeneration, with different possible applications. This membrane may be suitable as internal guiding cue inside tubular nerve conduits, to function as an adherent platform for Schwann cells and growing axons, at the same time that prevents excessive fibroblast infiltration. This kind of guidance has been described to be of fundamental importance when treating large gap defects. The DA III membrane material presents the right characteristics to be used straightaway with this purpose. Other possible application of the membrane may be as a basis for the construction of the tubular nerve guidance conduit itself, since the material can be easily rolled or wrapped. However, for this specific purpose, slight production modifications and further characterization would be required.

5. Conclusion

This extensive study aimed at providing a broad view on the suitability of chitosan membranes with three different degrees of acetylation (DA I: 1%, DA II: 2%, DA III: 5%) to support peripheral nerve regeneration. The surface and bulk properties of the three membranes are similar, indicating good suitability for peripheral nerve purposes, above all in the case the DA III formulation. The superior potential of the DA III membrane regarding PNR was confirmed by the biological studies, which showed higher proliferation and phenotypic expression of SCs cells when compared with DA I and DA II membranes. Interestingly, all the three formulations presented resistance to fibroblast adhesion and proliferation. In summary, this experimental work has led to the conclusion that DA III membrane should be the one considered for further PNR applications, since it will not induce calcification of the implant, excessive swelling or fibroblasts infiltration and it will allow a guided regeneration of the nerves mediated by preferential Schwann cell adhesion and proliferation.

Acknowledgments

This work has received funding from the European Community's Seventh Framework Programme (FP7-HEALTH-2011) under grant agreement no 278612 (BIOHYBRID). This study was also funded by European Union's FP7 Programme under grant agreement no REGPOT-CT2012-316331-POLARIS. The authors thank the chitosan raw material provided by Altakitin S.A., (Lisboa, Portugal). We are further thankful to Silke Fischer, Natascha Heidrich, Kerstin Kuhlemann, Jennifer Metzen, Hildegard Streich and Maike Wesemann (all from the Institute of Neuroanatomy, Hannover Medical School) for their technical support.

Appendix A. Supplementary data

Supplementary data to this article can be found online at http://dx.doi.org/10.1016/j.msec.2016.11.100.

References

[1] L.R. Robinson, Muscle Nerve 23 (2000) 863–873.
[2] J. Noble, C.A. Munro, V.S. Prasad, R. Midha, J. Trauma 45 (1998) 116–122.
[3] C.A. Taylor, D. Braza, J.B. Rice, T. Dillingham, Am. J. Phys. Med. Rehabil. 87 (2008) 381–385.
[4] W. Daly, L. Yao, D. Zeugolis, A. Windebank, A. Pandit, J. R. Soc. Interface 9 (2012) 202–221.
[5] W.Z. Ray, S.E. Mackinnon, J. Hand. Surg. [Am.] 36 (2011) 201–208.
[6] A.R. Nectow, K.G. Marra, D.L. Kaplan, Tissue Eng. B Rev. 18 (2012) 40–50.
[7] G.A.A. Saracino, D. Cigognini, D. Silva, A. Caprini, F. Gelain, Chem. Soc. Rev. 42 (2013) 225–262.
[8] J. Que, Q. Cao, T. Sui, S. Du, D. Kong, X. Cao, Cell Death Dis. 4 (2013) e526.
[9] W.C. Ngeow, Oral Surg. Oral Med. Oral Pathol. Oral Radiol. Endod. 109 (2010) 357–366.
[10] M.L. Ceci, C. Mardones-Krsulovic, M. Sanchez, L.E. Valdivia, M.L. Allende, Neural Dev. 9 (2014) 22.
[11] R.P. Bunge, J. Neurol. 242 (1994) S19–S21.
[12] S. Madduri, B. Gander, J. Peripher. Nerv. Syst. 15 (2010) 93–103.
[13] A.M. Agrawal, R.V. Manek, W.M. Kolling, S.H. Neau, J. Pharm. Sci. 93 (2004) 1766–1779.
[14] S. Gnavi, C. Barwig, T. Freier, K. Haastert-Talini, C. Grothe, S. Geuna, Chapter one - the use of chitosan-based scaffolds to enhance regeneration in the nervous system, in: I. Perroteau, P. Tos, S. Geuna, B. Bruno (Eds.), Int Rev Neurobiol, Academic Press, 2013, pp. 1–62.
[15] F. Gonzalez-Perez, S. Cobianchi, S. Geuna, C. Barwig, T. Freier, E. Udina, X. Navarro, Microsurgery 35 (2015) 300–308.

UNCORRECTED PROOF

[16] K. Haastert-Talini, S. Geuna, L.B. Dahlin, C. Meyer, L. Stenberg, T. Freier, C. Heimann, C. Barwig, L.F. Pinto, S. Raimondo, G. Gambarotta, S.R. Samy, N. Sousa, A.J. Salgado, A. Ratzka, S. Wrobel, C. Grothe, Biomaterials 34 (2013) 9886–9904.
[17] S. Wrobel, S.C. Serra, S. Ribeiro-Samy, N. Sousa, C. Heimann, C. Barwig, C. Grothe, A.J. Salgado, K. Haastert-Talini, Tissue Eng. A 20 (2014) 2339–2349.
[18] Y. Luo, Q. Wang, Int. J. Biol. Macromol. 64C (2014) 353–367.
[19] M.H. Cho, K.S. Kim, H.H. Ahn, M.S. Kim, S.H. Kim, G. Khang, B. Lee, H.B. Lee, Tissue Eng. A 14 (2008) 1099–1108.
[20] D. Ren, H. Yi, W. Wang, X. Ma, Carbohydr. Res. 340 (2005) 2403–2410.
[21] L.-Y. Zheng, J.-F. Zhu, Carbohydr. Polym. 54 (2003) 527–530.
[22] S. Chatterjee, A.K. Guha, Lett. Appl. Microbiol. 59 (2014) 155–160.
[23] M. Ignatova, K. Kalinov, N. Manolova, R. Toshkova, I. Rashkov, M. Alexandrov, J. Biomater. Sci. Polym. Ed. 25 (2014) 287–306.
[24] X. Xu, Y. Li, Y. Shen, S. Guo, Int. J. Biol. Macromol. 62 (2013) 418–425.
[25] C. Chatelet, O. Damour, A. Domard, Biomaterials 22 (2001) 261–268.
[26] T. Freier, H.S. Koh, K. Kazazian, M.S. Shoichet, Biomaterials 26 (2005) 5872–5878.
[27] R. Lieder, M. Darai, M.B. Thor, C.H. Ng, J.M. Einarsson, S. Gudmundsson, B. Helgason, V.S. Gaware, M. Masson, J. Gislason, G. Orlygsson, O.E. Sigurjonsson, J. Biomed. Mater. Res. A 100 (2012) 3392–3399.
[28] E.L. Mogilevskaya, T.A. Akopova, A.N. Zelenetskii, A.N. Ozerin, Polym. Sci. Ser. A 48 (2005) 216–226.
[29] M. Prasitsilp, R. Jenwithisuk, K. Kongsuwan, N. Damrongchai, P. Watts, J. Mater. Sci. Mater. Med. 11 (2000) 773–778.
[30] C. Wenling, J. Duohui, L. Jiamou, G. Yandao, Z. Nanming, Z. Xiufang, J. Biomater. Appl. 20 (2005) 157–177.
[31] I.F. Amaral, M. Lamghari, S.R. Sousa, P. Sampaio, M.A. Barbosa, J. Biomed. Mater. Res. A 75 (2005) 387–397.
[32] I.F. Amaral, A.L. Cordeiro, P. Sampaio, M.A. Barbosa, J. Biomater. Sci. Polym. Ed. 18 (2007).
[33] S.M. Lim, D.K. Song, K.J. Cho, S.H. Oh, D.S. Lee-Yoon, E.H. Bae, J.H. Lee, Cell adhesion and degradation behaviors of acetylated chitosan films, in: F. Ibrahim, N.A.A. Osman, J. Usman, N.A. Kadri (Eds.), 3rd Kuala Lumpur International Conference on Biomedical Engineering 2006: Biomed 2006, 11–14 December 2006 Kuala Lumpur, Malaysia, Springer, Berlin, Heidelberg, 2007, pp. 94–97.
[34] D.K. Owens, R.C. Wendt, J. Appl. Polym. Sci. 13 (1969) 1741–1747.
[35] T. Kokubo, H. Takadama, Biomaterials 27 (2006) 2907–2915.
[36] H. Baniasadi, S.A.A. Ramazani, S. Mashayekhan, Int. J. Biol. Macromol. 74 (2015) 360–366.
[37] Y. Wang, Y. Zhao, C. Sun, W. Hu, J. Zhao, G. Li, L. Zhang, M. Liu, Y. Liu, F. Ding, Y. Yang, X. Gu, Mol. Neurobiol. (2014).
[38] H.-I. Chang, Cell Responses to Surface and Architecture of Tissue Engineering Scaffolds, InTech, 2011.
[39] K.J. Kubiak, M.C. Wilson, T.G. Mathia, S. Carras, Scanning 33 (2011) 370–377.
[40] J.H. Choee, S.J. Lee, Y.M. Lee, J.M. Rhee, H.B. Lee, G. Khang, J. Appl. Polym. Sci. 92 (2004) 599–606.
[41] A. Sethuraman, M. Han, R.S. Kane, G. Belfort, Langmuir 20 (2004) 7779–7788.
[42] H.-C. Lai, L.-F. Zhuang, X. Liu, M. Wieland, Z.-Y. Zhang, Z.-Y. Zhang, J. Biomed. Mater. Res. A 93A (2010) 289–296.
[43] H.K. Dhiman, A.R. Ray, A.K. Panda, Biomaterials 25 (2004) 5147–5154.
[44] Y. Wan, K.A.M. Creber, B. Peppley, V.T. Bui, Polymer 44 (2003) 1057–1065.
[45] Y.W. Cho, J. Jang, C.R. Park, S.W. Ko, Biomacromolecules 1 (2000) 609–614.
[46] J. Li, J. Revol, R.H. Marchessault, J. Colloid Interface Sci. 192 (1997) 447–457.
[47] I. Younes, M. Rinaudo, Mar. Drugs 13 (2015) 1133–1174.
[48] M.A. Gamiz-Gonzalez, A.E. Piskin, C. Pandis, C. Chatzimanolis-Moustakas, A. Kyritsis, B. Mari, J.L. Ribelles, A. Vidaurre, Carbohydr. Polym. 133 (2015) 110–116.
[49] S.F. Wang, L. Shen, Y.J. Tong, L. Chen, I.Y. Phang, P.Q. Lim, T.X. Liu, Polym. Degrad. Stab. 90 (2005) 123–131.
[50] P.P. Dhawade, R.N. Jagtap, Adv. Appl. Sci. Res. 3 (2012) 1372–1382.
[51] L.S. Guinesi, É.T.G. Cavalheiro, Thermochim. Acta 444 (2006) 128–133.
[52] M.B. Steed, V. Mukhatyar, C. Valmikinathan, R.V. Bellamkonda, Atlas Oral Maxillofac. Surg. Clin. North Am. 19 (2011) 119–130.
[53] R.J. Nordtveit, K.M. Vårum, O. Smidsrød, Carbohydr. Polym. 29 (1996) 163–167.
[54] H. Millesi, G. Zoch, R. Reihsner, Clin. Orthop. Relat. Res. (1995) 76–83.
[55] D.F. Meaney, Clin. Podiatr. Med. Surg. 12 (1995) 363–384.
[56] J.M. Sobral, S.G. Caridade, R.A. Sousa, J.F. Mano, R.L. Reis, Acta Biomater. 7 (2011) 1009–1018.
[57] J.F. Mano, Macromol. Biosci. 8 (2008) 69–76.
[58] S. Ghosh, V. Gutierrez, C. Fernández, M.A. Rodriguez-Perez, J.C. Viana, R.L. Reis, J.F. Mano, Acta Biomater. 4 (2008) 950–959.
[59] L.-P. Yan, Y.-J. Wang, L. Ren, G. Wu, S.G. Caridade, J.-B. Fan, L.-Y. Wang, P.-H. Ji, J.M. Oliveira, J.T. Oliveira, J.F. Mano, R.L. Reis, J. Biomed. Mater. Res. A 95A (2010) 465–475.
[60] A.I. Teixeira, S. Ilkhanizadeh, J.A. Wigenius, J.K. Duckworth, O. Inganas, O. Hermanson, Biomaterials 30 (2009) 4567–4572.
[61] L.A. Flanagan, Y.E. Ju, B. Marg, M. Osterfield, P.A. Janmey, Neuroreport 13 (2002) 2411–2415.
[62] L. Ning, Y. Xu, X. Chen, D.J. Schreyer, J. Biomater. Sci. Polym. Ed. 27 (2016) 898–915.
[63] G.H. Borschel, K.F. Kia, W.M. Kuzon Jr, R.G. Dennis, J. Surg. Res. 114 (2003) 133–139.
[64] L. Zilic, P.E. Garner, T. Yu, S. Roman, J.W. Haycock, S.-P. Wilshaw, J. Anat. 227 (2015) 302–314.
[65] L. Zilic, S.-P. Wilshaw, J.W. Haycock, Biotechnol. Bioeng. 113 (2016) 2041–2053.
[66] A.S. Kulshrestha, A. Mahapatro, L.A. Henderson, ACS Symposium Series, American Chemical Society, 20100.
[67] J.P.F. Wong, D. Baptista, R.A. Brown, Acta Biomater. 10 (2014) 5005–5011.
[68] J.W. Gunn, S.D. Turner, B.K. Mann, J. Biomed. Mater. Res. A 72 (2005) 91–97.
[69] S.A. Mobasseri, G. Terenghi, S. Downes, J. Mater. Sci. Mater. Med. 24 (2013) 1639–1647.
[70] M. Sun, S. Downes, J. Mater. Sci. Mater. Med. 20 (2009) 1181–1192.
[71] A.C. de Luca, G. Terenghi, S. Downes, J. Tissue Eng. Regen. Med. 8 (2014) 153–163.
[72] U. Namgung, Cells Tissues Organs 200 (2014) 6–12.
[73] S. Atkins, K.G. Smith, A.R. Loescher, F.M. Boissonade, S. O'Kane, M.W. Ferguson, P.P. Robinson, Neuroreport 17 (2006) 1245–1249.
[74] J.S. Park, J.H. Lee, C.S. Han, D.W. Chung, G.Y. Kim, Clin. Orthop. Surg. 3 (2011) 315–324.
[75] B. Martinac, J. Cell Sci. 117 (2004) 2449–2460.
[76] N.F. Berbari, A.K. O'Connor, C.J. Haycraft, B.K. Yoder, Curr. Biol. 19 (2009) R526–R535.
[77] C.G. Galbraith, K.M. Yamada, M.P. Sheetz, J. Cell Biol. 159 (2002) 695–705.
[78] C.A. Reinhart-King, M. Dembo, D.A. Hammer, Biophys. J. 89 (2005) 676–689.
[79] B.C. Isenberg, P.A. Dimilla, M. Walker, S. Kim, J.Y. Wong, Biophys. J. 97 (2009) 1313–1322.
[80] K.R. Levental, H. Yu, L. Kass, J.N. Lakins, M. Egeblad, J.T. Erler, S.F. Fong, K. Csiszar, A. Giaccia, W. Weninger, M. Yamauchi, D.L. Gasser, V.M. Weaver, Cell 139 (2009) 891–906.
[81] C.M. Lo, H.B. Wang, M. Dembo, Y.L. Wang, Biophys. J. 79 (2000) 144–152.

UNCORRECTED PROOF